JOURNAL OF Materials CHEMISTRY

Sorption characteristics of radionuclides on synthetic birnessite-type layered manganese oxides

Alan Dyer,*[a] Martyn Pillinger,[a] Risto Harjula[b] and Suheel Amin[c]

[a]*Chemistry Division, Science Research Institute, Cockcroft Building, University of Salford, Salford, UK M5 4WT. E-mail: a.dyer@salford.ac.uk*
[b]*Laboratory of Radiochemistry, Department of Chemistry, PO Box 55, University of Helsinki, Finland FI-00014*
[c]*British Nuclear Fuels plc, Risley, Warrington, Cheshire, UK WA3 6AS*

Received 28th March 2000, Accepted 12th June 2000
Published on the Web 12th July 2000

The removal of trace caesium (^{137}Cs), trace strontium (^{89}Sr, ^{90}Sr/^{90}Y) and trace cobalt (^{57}Co) from aqueous solution by synthetic sodium and potassium birnessites has been studied by a batch technique. Distribution coefficients were determined as a function of pH in four solutions: water, 0.005 M sodium tetraborate, 0.005 M sodium citrate and 0.0001 M EDTA. Other effects studied were increasing sodium ion, potassium ion and complexing agent concentration. Key synthesis parameters (ageing time, MnO_4^-/Mn^{2+} ratio) were tuned in order to maximise trace cobalt sorption efficiencies. The optimised material was tested for the removal of caesium, strontium and cobalt from a nuclear power plant floor drain simulant. A sodium birnessite sample was also screened for the removal of ^{63}Ni, ^{54}Mn, ^{59}Fe, ^{65}Zn and ^{236}Pu radionuclides.

Introduction

There is a continuing need to develop new ion-exchange materials for the remediation of aqueous radioactive wastes arising from nuclear power stations, military sites, reprocessing plants, and research centres. Many of these waste solutions are extremely challenging as they are either highly alkaline or highly acidic with very high salt concentrations, and may also contain complexing agents. Porous inorganic crystals with layered and tunnel structures have attracted considerable interest as potential sorbents, as they often have high capacities and selectivities for certain monovalent and divalent cations.[1] New materials are discovered regularly, some of which are analogues of natural minerals, while others have novel structures. Examples of layered compounds include alkali metal titanates, titanoniobates, niobates and manganates.

An ion exchange–ceramic process has been developed for the treatment of nuclear waste. After use in column operations, the ion exchanger is vitrified, or encapsulated in cement, for long-term disposal as high-level waste in deep underground repositories, whereas the larger volume of remaining material is more easily disposed of as low-level waste. Synthetic inorganic layered materials that have been investigated for this task include sodium titanates,[2] titanium phosphates[3] and micas.[4,5] Radionuclides of interest include the fission products ^{137}Cs ,^{90}Sr, and ^{60}Co. The latter isotope is also formed by neutron activation of ^{59}Co present as an impurity in stainless steel. Another potential use of layered materials in this process is as adsorbents to back-fill the sealed repository. Clay minerals such as bentonite and montmorillonite have been proposed for this purpose.[6–8] More generally, the sorption of radionuclides on natural materials is important for the prediction of migration rates of radionuclides in the formations near geological storage sites.

Birnessite is a naturally occurring layered manganese oxide that exists in a wide variety of soil and marine environments. It is an important ion exchange material,[9–15] a precursor to todorokite (a tunnel manganese oxide containing 3×3 MnO_6 units),[16–18] and plays an important role in the distribution of heavy metals, particularly cobalt, in soil and marine environments.[19–22] Numerous methods have been developed to synthesise birnessite in the laboratory.[9,10,12,16,17,23] The structure of Na-birnessite consists of sheets of edge-sharing MnO_6 octahedra separated by exchangeable Na and water.[24,25] The basal spacing may be 7 Å (birnessite, single crystal water sheet) or 10 Å (buserite, double crystal water sheet). Birnessite behaves as an ion-sieve material with an effective pore diameter of 3 Å.[14]

As part of a programme to develop crystalline synthetic inorganic ion exchangers for radioactive waste volume minimisation,[26,27] the present study describes the sorption behaviour of synthetic layered manganese oxides for the separation of trace caesium (^{137}Cs), strontium (^{89}Sr, ^{90}Sr/^{90}Y) and cobalt (^{57}Co) ions from aqueous solutions containing competing ions (Na^+, K^+, Mg^{2+}, Ca^{2+}, H^+) and complexing agents (EDTA, tetraborate, citrate) of interest in radionuclide-bearing waste effluents. Synthesis conditions were varied systematically in order to maximise sorption efficiencies. Screening tests were also carried out for the removal of ^{63}Ni, ^{54}Mn, ^{59}Fe, ^{65}Zn and ^{236}Pu radionuclides.

Experimental

Chemicals used were of reagent grade quality and were obtained from commercial sources without further purification. Radioisotopes were supplied by Amersham International, Amersham, UK.

Preparation of Na-birnessite samples[16,17]

A $Mn(OH)_2$ sol was prepared by addition of 5.0 M NaOH (100 mL) to 0.5 M $MnCl_2 \cdot 4H_2O$ (80 mL) at room temperature with vigorous stirring. It was then added dropwise to different amounts of 0.093 M $Mg(MnO_4)_2 \cdot 6H_2O$ at room temperature with vigorous stirring [$MnO_4^-/Mn^{2+} = 0.30$, 0.33, 0.37, 0.4]. The resulting suspensions (pH 13.7) were aged at room temperature for 7 days, then filtered, washed with double distilled water (DDW), and air-dried at ambient temperature. Four other samples were prepared with $MnO_4^-/Mn^{2+} = 0.40$ and ageing times of 0.83, 7, 14 and 21 days. Sample abbreviations and analytical data are given in Table 1.

Two potassium form layered manganese oxide materials

Table 1 Analytical data for Na-birnessites (Na-B) and K-birnessites (K-B)

Sample	MnO_4^-/Mn^{2+}	Ageing time /days	Mn (%)	Na or K (%)	H_2O (%)	Z_{Mn}[a]
Na-B1	0.30	7	48.97	3.82	18.4	3.33
Na-B2	0.33	7	45.06	4.52	20.1	3.46
Na-B3	0.37	7	50.06	5.47	18.4	3.44
Na-B4	0.40	7	46.32	5.28	19.6	3.57
Na-B5	0.40	1	47.49	4.66	17.3	3.47
Na-B6	0.40	7	46.62	5.46	17.0	3.58
Na-B7	0.40	14	46.67	6.22	18.2	3.47
Na-B8	0.40	21	46.19	6.11	17.6	3.56
K-B1	0.33	7	51.07	5.02	—	3.41
K-B2	0.40	7	48.54	6.88	—	3.57

[a] Z_{Mn} = Average manganese oxidation state.

were also prepared using the above method, using KOH instead of NaOH. The ageing time was 7 days with $MnO_4^-/Mn^{2+} = 0.33$ and 0.40 (Table 1).

Physical analyses

Powder X-ray diffraction (XRD) patterns were collected on a Siemens D5000 diffractometer with Cu-Kα radiation. Water contents in samples pre-equilibrated over saturated NaCl for 1 week were determined by thermogravimetry (TGA) using a Mettler TA3000 system at a heating rate of 5 K min^{-1} under a nitrogen atmosphere.

Chemical analyses

Elemental chemical analyses for sodium, potassium and manganese were performed by atomic absorption spectroscopy (AAS). About 50 mg of sample was dissolved with 20 mL double distilled water (DDW), 1 mL of concentrated nitric acid, and 2 mL of 30% hydrogen peroxide. The colourless solution was boiled for 2–5 min to remove excess peroxide and the solution was diluted with DDW to 100 mL to make a stock solution.

Average manganese oxidation states were determined using the standard oxalic acid–permanganate back-titration procedure. About 0.2 g of each sample was weighed out and transferred into a 250 mL Erlenmeyer flask containing a 50 mL solution of 10% H_2SO_4 mixed with 0.5 g of $Na_2C_2O_4$. With mild heating ($<100\,^{\circ}C$), the samples dissolved completely. $KMnO_4$ solution (0.02 M, standardised by $Na_2C_2O_4$ according to the standard method) was then used to back-titrate the excess $Na_2C_2O_4$.

Sorption experiments

Distribution coefficients were determined by the batch method using radioactive tracer ions. Between 25 and 50 mg of exchanger were equilibrated at ambient temperature with spiked solutions in 15 mL polyethylene centrifuge tubes (Elkay) or 20 mL polyethylene vials (Zinsser) by end over end tumbling in a mineralogical roller. Contact times of 1 to 2 days were used. In the "carrier-free" experiments, the concentration of caesium was in the range 2.0×10^{-8}–3.7×10^{-7} M, the concentration of strontium was in the range 1.5–3.1×10^{-6} M, and the concentration of cobalt was in the range 3.6–7.3×10^{-11} M. ^{57}Co tracer, which has a high specific activity, was used to avoid precipitation of cobalt hydroxide in alkaline solutions. The solutions were separated from the solids by centrifugation (15 min at 4000 or 30 000 G) followed by filtration through a 0.22 μm polyvinyldifluoride membrane (no filtration in the case of ^{236}Pu). Tracer activities in solution were measured using either a NaI crystal and a single-channel analyser (^{57}Co, ^{65}Zn, ^{54}Mn and ^{59}Fe) or a Canberra-Packard 1900 CA tri-Carb liquid scintillation counter (^{236}Pu, ^{89}Sr, $^{90}Sr/^{90}Y$, ^{57}Co and ^{137}Cs). Blank determinations were also carried out in order to make corrections for adsorption on contact vials and filters, and to check for possible precipitation of radionuclides. Filtrates from all ion exchange experiments were measured using an Orion model 720A pH meter fitted with an Accumet semi micro calomel electrode.

The distribution coefficient (K_d) was calculated as follows where A_i and A are the tracer activities before and after treatment, respectively, V is the solution volume (mL) and m is the mass (g) of the manganese oxide.

$$K_d = \frac{(A_i - A)}{A}\frac{V}{m} = \frac{\text{Concentration of ion in exchanger}}{\text{Concentration of ion in solution}} \quad (1)$$

The K_d calculations were based on the hydrated weight of the exchanger. In determining K_d as a function of pH, the pH was adjusted by adding concentrated HNO_3 to the solution/exchanger mixture. Prior to the experiments to study the effect of complexants on trace ion sorption efficiencies, freshly prepared solutions of trisodium citrate, sodium tetraborate and EDTA (disodium dihydrogenethylenediaminetetraacetate) were spiked with the radioactive tracer and left to stand at room temperature for 3 days to allow complete complexation.

Theory

A binary ion exchange reaction between ion A (charge z_A) and ion B (charge z_B) may be written in terms of eqn. (2)

$$z_B A^{z_A+} + z_A \bar{B}^{z_B+} \leftrightarrow z_A B^{z_B+} + z_B \bar{A}^{z_A+} \quad (2)$$

where over-bars refer to the ions in the ion exchanger. The selectivity coefficient is then given by eqn. (3)

$$K_{A/B} = \frac{\bar{C}_A^{z_B} C_B^{z_A}}{\bar{C}_B^{z_A} C_A^{z_B}} \quad (3)$$

where the $\bar{C}$ values are the concentrations of the ions in the exchanger and C values those in the solution. From eqn. (1) ($K_d = \bar{C}_A/C_A$) and eqn. (3) one obtains eqn. (4).

$$K_d = K_{A/B}^{1/z_B}\left(\frac{\bar{C}_B}{C_B}\right)^{\frac{z_A}{z_B}} \quad (4)$$

Under the special condition that A is present in solution and in the exchanger at much lower concentration than B ($\bar{C}_A \ll \bar{C}_B$, $C_A \ll C_B$, *e.g.*, when A is a trace caesium ion and B is a macro-ion such as sodium), $K_{A/B}$ and $\bar{C}_B$ are practically constant ($\bar{C}_B \approx Q$, the ion exchange capacity) and one obtains eqn. (5) which indicates that a plot of log K_d against log C_B should give a straight line with slope $-z_A/z_B$.[28,29]

$$\log K_d = \frac{1}{z_B}\log(K_{A/B}Q^{z_A}) - \frac{z_A}{z_B}\log C_B \quad (5)$$

However, the overriding condition for linear dependence becomes apparent if, for simplicity, a binary uni-univalent exchange is considered ($z_A = z_B = 1$). Inserting $\bar{C}_B = Q - \bar{C}_A$ into eqn. (3) and combining with $K_d = \bar{C}_A / C_A$ gives eqn. (6).

$$K_d = \frac{Q}{\frac{C_B}{K_{A/B}} + C_A} \quad (6)$$

This shows that the condition for linear dependence is in fact $C_B / K_{A/B} \gg C_A$.

Results and discussion

Birnessite-type manganese oxides can be expressed by the general formula $(A_x)[\square_z Mn^{III}_y Mn^{IV}_{1-y-z}]O_2 \cdot nH_2O$ where ( ), [ ], □ and A are interlayer sites, octahedral sites on the MnO_6 sheet, vacancies on the MnO_6 sheet, and metal ions in the interlayer sites, respectively, and x can be up to 0.7 for Na-birnessite.[9] EXAFS studies have indicated that there are two types of sites for metal ions locating in the interlayer.[25] One site (A) is located on the crystal water sheet, and the other (B) located above and below the vacancies on the MnO_6 sheets. The alkali and alkaline earth metal ions with large ionic radii (unhydrated) are located in A sites, and transition metal ions with small ionic radii (*e.g.*, Zn^{2+}, Cu^{2+}, Ni^{2+}, Co^{2+} and Mn^{2+}) are located at the B sites.

The layered manganese oxide samples used in this work were prepared using a literature method that involves the oxidation of $Mn(OH)_2$ in MOH (M = Na, K) by $Mg(MnO_4)_2$, and ageing the resulting gel at room temperature (Table 1).[16,17] Important synthesis parameters are the MnO_4^-/Mn^{2+} ratio, basicity, crystallisation time and temperature. Suib and co-workers showed that, using this method, crystalline birnessite-type materials are obtained with a MnO_4^-/Mn^{2+} ratio between 0.3 and 0.4, the optimum crystallisation time being 7 days.[16] In the work presented here, different samples were prepared by either varying the MnO_4^-/Mn^{2+} ratio, with an ageing time of 7 days, or by varying the crystallisation time, with a MnO_4^-/Mn^{2+} ratio of 0.4 (Table 1). The average manganese oxidation states of the products were determined, and increased from 3.3 to 3.6 as the MnO_4^-/Mn^{2+} ratio was increased from 0.3 to 0.4. For samples Na-B1 to Na-B4, three major peaks were observed in the powder XRD pattern at 7.28, 4.66 and 3.55 Å, similar to that reported previously.[16] For samples K-B1 and K-B2, three major peaks were observed at 7.13, 4.62 and 3.54 Å.

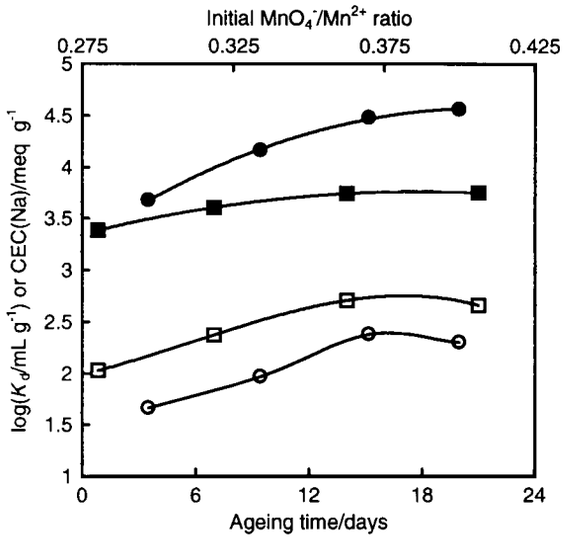

Fig. 1 Distribution coefficient of ^{57}Co on Na-birnessites (■) and the corresponding sodium cation exchange capacity (CEC) of the materials (□) as a function of ageing time, and distribution coefficient of ^{57}Co on Na-birnessites (●) and the corresponding sodium CEC (○) as a function of MnO_4^-/Mn^{2+} ratio ($V/m = 200$ mL g^{-1}).

Fig. 1 shows the distribution coefficient (K_d) of trace cobalt (^{57}Co) on manganese oxide samples Na-B1 to Na-B8, at either equilibrium pH 3 in 0.1 M $NaNO_3$ for samples prepared with different MnO_4^-/Mn^{2+} ratios, or in 0.1 M HNO_3 (equilibrium pH 1.24) for samples prepared with different crystallisation times. Also plotted are the corresponding sodium cation exchange capacities (CEC) for each of the materials. It is clear that sodium CECs and sorption efficiencies for trace cobalt increase with both ageing time and MnO_4^-/Mn^{2+} ratio. The uptake of cobalt is particularly dependent on the last parameter. With $MnO_4^-/Mn^{2+} = 0.3$, a K_d of 5280 mL g^{-1} (96.4% sorption) was achieved at pH 3 in 0.1 M $NaNO_3$, while with $MnO_4^-/Mn^{2+} = 0.4$, a K_d of 36850 mL g^{-1} (99.5% sorption) was achieved under the same conditions. The plot of sodium content against ageing time reveals the three stages in the crystallisation of birnessite: an induction period (1–2 days), a fast crystallisation period (2–12 days), when the CEC increases linearly, and a steady-state period, when the CEC becomes almost constant.[23] The results show that the best material for the removal of cobalt is obtained with a MnO_4^-/Mn^{2+} ratio of 0.4 and ageing time of 2 weeks, and can be formulated as $Na_{4.3}Mn_{14}O_{27} \cdot 16H_2O$. This material gave a ^{57}Co K_d of 5500 mL g^{-1} in 0.1 M HNO_3 (final pH 1.24), which with a batch factor of 200 means 96.5% cobalt ion sorption. Other reported sorbents such as clay minerals,[6a] a hydrous manganese oxide,[30,31] activated carbons,[32] natural magnetite and hematite,[33] take up virtually no radiocobalt under the same conditions.

There is an increasing demand for the selective removal of other activated corrosion product nuclides in addition to ^{60}Co (^{65}Zn, ^{54}Mn, ^{59}Fe, ^{63}Ni, ^{51}Cr) at nuclear power plants. The Na-birnessite sample Na-B3 was tested for the removal of some of these radionuclides and also ^{236}Pu in four test solutions (Table 2). Very high distribution coefficients were obtained for all radionuclides in distilled water (pH 10.8) and in 0.1 M $NaNO_3$ (pH 9.1). Significantly, the uptake of ^{236}Pu in 0.1 M $NaNO_3$ and distilled water (*ca.* 99.7%) was higher than that attained in 0.1 M $NaNO_3$/0.1 M NaOH (94%). Even in 0.1 M HNO_3 a reasonable ^{236}Pu K_d of 49 mL g^{-1} was obtained (33% sorption). The equilibrium pH observed in distilled water indicates that significant hydrolysis of the exchanger took place [eqn. (7)]. The pH decreased in 0.1 M $NaNO_3$, because increasing sodium ions in solution cause a shift to the left in reaction (7).

$$Na\text{–}B + H_2O \Leftrightarrow H\text{–}B + Na^+ + OH^- \quad (7)$$

It is worth noting that for all radionuclides distribution coefficients in 0.1 M $NaNO_3$ were at least as high or higher than those attained in distilled water, and always higher than those attained in 0.1 M $NaNO_3$/0.1 M NaOH. The strong preference for transition metal cations such as Zn is in accord with that observed for soil manganese oxides by McKenzie,[34] and by Loganathan and Burau for synthetic δ-MnO_2 (a hydrous manganese oxide similar to birnessite).[20] The adsorption capacity of the K^+-form δ-MnO_2 was reported to increase in the series: $Ni^{2+} < Co^{2+} < Cd^{2+} \approx Zn^{2+} < Mn^{2+}$.[11]

An ion exchange mechanism has been proposed for the adsorption of alkaline-earth and heavy metal cations on δ-MnO_2.[11] However, the adsorption of heavy metal cations is expected to be more complex than the adsorption of alkaline-earth cations because of the formation of hydrolysis products of the heavy metal cations at lower pH values than the alkaline-earth cations and also because some of the cations may displace Mn ions from the lattice of MnO_2 (discussed below in more detail for cobalt). Very little radiocobalt was removed from 0.1 M $NaNO_3$/0.1 M NaOH which can be attributed to the formation of $Co^{II}(OH)^+$, soluble $Co^{II}(OH)_2$ and $Co^{II}(OH)_3^-$.

Table 2 Distribution coefficients (mL g^{-1}) of radionuclides on Na-birnessite (Na-B3) in different solutions (equilibrium pH in parentheses)

	V/*m*	Distilled H_2O (10.8)	0.1 M $NaNO_3$ (9.1)	0.1 M $NaNO_3$ 0.1 M NaOH	0.1 M HNO_3 (1.2)
^{57}Co	200	46 900	446 000	0	2530
^{65}Zn	200	384 000	>1 000 000	69 930	55
^{54}Mn	200	>1 000 000	364 000	4050	55
^{59}Fe	200	>1 000 000	>1 000 000	127 000	50 300
^{236}Pu	100	27 740	39 700	1620	49

In the case of Fe^{2+}, the dominant sorption mechanism probably involves oxidation of Fe^{2+} to Fe^{3+} either on the surface of the manganese oxide or in the interlayer, with concomitant liberation of Mn^{2+}. Iron oxide will precipitate except possibly at pH < 2. Even at pH 1, the material was very specific for ^{59}Fe (K_d = 50 000, 99.6% sorption).

Fig. 2 shows the distribution coefficients of ^{137}Cs, ^{89}Sr and ^{57}Co on Na-B2 as a function of sodium ion concentration. In the concentration range 0.03–1.0 M the ^{137}Cs and ^{89}Sr K_ds decrease linearly on a logarithmic scale with slopes of −0.82 (intercept 0.20) and −1.40 (intercept 2.66) respectively, indicating that both trace caesium and trace strontium are taken up by an ion exchange mechanism [eqn. (5)]. The former value is close to that expected for exchange of a univalent ion for a univalent ion, *i.e.*, exchange of caesium ions for sodium ions at site A located on the crystal water sheet. A slope of −2 would be expected for exchange of divalent strontium ions for sodium ions. The observed value of −1.4 may be attributed to the fact that the equilibrium pH is slightly alkaline even up to $[Na^+]$ = 1.0 M and therefore the presence of the hydrolysed species of strontium, $Sr(OH)^+$, distorts the ideal picture. Selectivity coefficients for trace caesium and trace strontium exchange were determined from the linearly declining parts of the curves in Fig. 2, using eqn. (5). Values of 1 and 75 were obtained for the ion pairs Cs/Na and Sr/Na respectively. In 1.0 M $NaNO_3$ practically no caesium was taken up by the exchanger, while uptake of trace strontium was still quite high (82%). At low initial sodium ion concentrations the distribution coefficients of ^{137}Cs and ^{89}Sr level off to constant values. This phenomenon has been observed previously with other weak acid inorganic ion exchangers such as layered sodium titanates[2] and framework titanium silicates,[26,27] and can be attributed to hydrolysis of the exchanger, which brings a constant sodium ion concentration into the solution.

The sorption behaviour of ^{57}Co on Na-B2 was quite different from that of ^{137}Cs and ^{89}Sr in that the distribution coefficient appears to be independent of sodium ion concentration, at least up to $[Na^+]$ = 1.0 M (Fig. 2). At this high salt concentration the sorption of trace cobalt was still 99.97%. This is consistent with the view that exchange of cobalt ions for sodium ions at the A sites is not the determining factor in the sorption process. For this to be the case, the equilibrium would have to be very favourable, *i.e.*, a selectivity coefficient so large that the distribution coefficient only depends on the concentration of cobalt ions in solution, and not on the concentration of sodium ions [eqn. (6)]. Instead, the likely sorption mechanism involves exchange of Co^{2+} ions for Mn^{2+} ions at the B sites located above and below vacancies in the MnO_6 sheet. It was reported that approximately 1 in 20 layer octahedral sites were vacant in a synthetic 7 Å birnessite.[25]

The distribution coefficients of ^{137}Cs, $^{90}Sr/^{90}Y$ and ^{57}Co on K-birnessite (K-B1) were determined as a function of potassium ion concentration (Fig. 3). The performance for each of the respective radionuclides was very similar to that achieved by Na-B2 in sodium nitrate solutions. Above a potassium ion concentration of 0.01 M the ^{137}Cs K_d decreased linearly on a logarithmic scale with a slope of −1.13 (intercept −0.46), close to the theoretical value of −1 for exchange of a univalent ion for a univalent ion. A selectivity coefficient of 0.3 was calculated using eqn. (5). In the concentration range 0.001–1.0 M, the K_d of $^{90}Sr/^{90}Y$ was approximately four orders of magnitude higher than that of ^{137}Cs at any given concentration, very similar to that observed for ^{89}Sr on Na-B2 in sodium nitrate solutions.

The sorption behaviour of ^{137}Cs, ^{89}Sr and ^{57}Co on Na-birnessite (Na-B2) was determined as a function of pH (Fig. 4). As the pH is lowered, the proportion of the exchanger in the hydrogen form increases. The sorption behaviour of ^{89}Sr as a function of pH resembles that observed for other weak acid inorganic exchangers with layered and tunnel structures, for

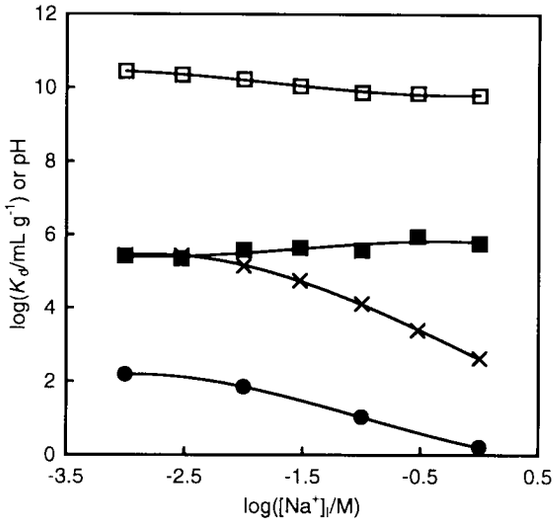

Fig. 2 Distribution coefficients of ^{137}Cs (●), ^{89}Sr (×) and ^{57}Co (■) on Na-birnessite (Na-B2), and the corresponding equilibrium pH (□) as a function of sodium ion ($NaNO_3$) concentration (*V*/*m* = 100 mL g^{-1} for ^{137}Cs and ^{89}Sr, 200 mL g^{-1} for ^{57}Co).

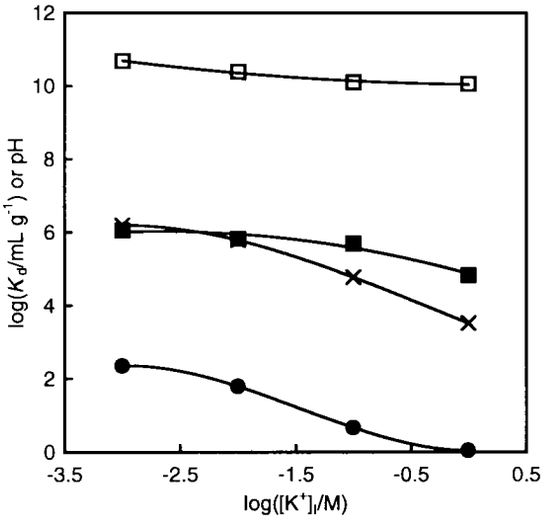

Fig. 3 Distribution coefficients of ^{137}Cs (●), ^{89}Sr (×) and ^{57}Co (■) on K-birnessite (K-B1), and the corresponding equilibrium pH (□) as a function of potassium ion (KNO_3) concentration (*V*/*m* = 100 mL g^{-1} for ^{137}Cs and ^{89}Sr, 200 mL g^{-1} for ^{57}Co).

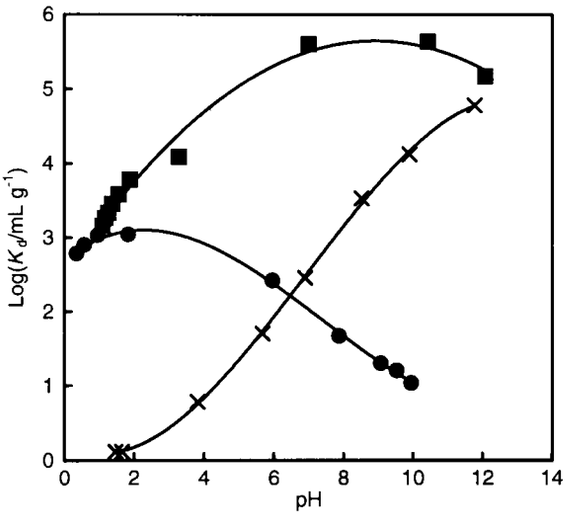

Fig. 4 Distribution coefficients of ^{137}Cs (●), ^{89}Sr (×) and ^{57}Co (■) on Na-B2 as a function of pH in plain water (^{57}Co, $V/m = 200$ mL g^{-1}) and in 0.1 M $NaNO_3$ (^{137}Cs and ^{89}Sr, $V/m = 100$ mL g^{-1}).

example sodium titanate,[2] and titanosilicate analogues of the minerals pharmacosiderite[26] and zorite.[27] Below pH 12 ($K_d = 10\,000$ mL g^{-1}) the K_d of ^{89}Sr decreased sharply, approximately linearly on a logarithmic scale, and at pH 1 practically no strontium was taken up by the exchanger. Almost the reverse was the case for ^{137}Cs. Thus, the ^{137}Cs K_d increased by about two orders of magnitude as the pH decreased from 10 to 2. This is very unusual behaviour for weak acid exchangers including hydrous manganese oxides. For example, Mikhail and Misak studied the adsorption of radiocaesium on a hydrous manganese oxide and found that uptake increased with an increase of solution pH, becoming almost constant at pH 4.5–8.5, and decreasing thereafter.[30] Their material was said to have a structure resembling that of γ-Mn_2O_3.[31] The peculiar behaviour observed for Na-B2 must be associated with a structural change occurring during the transformation of Na-birnessite to H-birnessite. The conversion of a synthetic Na-rich buserite to its low pH form, hexagonal H-birnessite, was recently investigated by Drits *et al.* using a combination of X-ray and selected area diffraction, and EXAFS.[25] The precursor had the composition $(Na_{0.3})[Mn^{IV}_{0.69}Mn^{III}_{0.31}]O_2$ and was free of layer vacancies. In acidic solution, disproportionation of layer Mn^{3+} occurs which causes formation of layer vacancies. The dissolved Mn^{2+} can be re-adsorbed at the B site of birnessite. H-birnessite synthesised at pH 4 had the composition $(Mn^{II}_{0.05}Mn^{III}_{0.116})[Mn^{IV}_{0.74}Mn^{III}_{0.093}\square_{0.167}]O_{1.70}(OH)_{0.3}$.

Na-B2 is highly effective at removing trace cobalt in the pH range 1–12 (Fig. 4). At pH 1, a ^{57}Co K_d of 1500 mL g^{-1} was achieved. Uptake increased with an increase of solution pH, becoming almost constant at pH 7–10 ($K_d = 450\,000$ mL g^{-1}), and decreased thereafter. It is generally accepted that the geochemical association between cobalt and manganese oxides results from the oxidation of highly soluble Co^{2+} species to weakly soluble Co^{3+} species, coupled with reduction of Mn^{4+} or Mn^{3+} ions, initially present in the manganese oxide sorbent, to soluble Mn^{2+}. The details of the sorption mechanism have been investigated by many groups over the years,[19–22] most recently by Manceau *et al.*[22] who prepared Co-sorbed samples at different surface coverages by equilibrating a Na-exchanged buserite suspension in the presence of aqueous Co^{2+} at pH 4. Two distinct oxidation mechanisms were identified that occured concurrently with the transformation of low pH monoclinic buserite to hexagonal H-rich birnessite. The first mechanism involves the sorption of divalent cobalt above or below a vacant layer site. It is then oxidised by the nearest layer Mn^{3+} and the resulting Co^{3+} species fills the vacant position in the layer while the reduced Mn migrates to the interlayer or into solution creating a new vacant site. The second oxidation mechanism involves the replacement of interlayer Mn^{3+} by interlayer Co^{3+}; the latter may eventually migrate into layer vacancies.

Synthetic organic complexing agents such as EDTA are used as cleaning agents and decontaminants at nuclear installations. Complexing agents such as citrate are present in soil and natural waters, and can arise from the breakdown of cellulosic materials such as tissues and clothing. The distribution coefficients of ^{137}Cs, ^{90}Sr/^{90}Y and ^{57}Co on Na-B2 were determined as a function of pH in 0.005 M sodium tetraborate (Fig. 5), 0.005 M sodium citrate (Fig. 6) and 0.0001 M disodium EDTA (Fig. 7). The overall sorption behaviour of ^{137}Cs and ^{90}Sr/^{90}Y on Na-B2 as a function of pH in 0.005 M sodium tetraborate does not differ significantly from that observed for ^{137}Cs and ^{89}Sr in 0.1 M $NaNO_3$, in the absence of the complexing agent (Fig. 5). It appears therefore that tetraborate anions do not have a marked suppressing effect on trace caesium and strontium sorption efficiencies. In fact, uptake was generally higher in 0.005 M sodium tetraborate than in 0.1 M $NaNO_3$, probably due to the different total sodium ion concentrations. By contrast, comparison of Figs. 4 and 5 shows that tetraborate anions interfere strongly in the removal of trace cobalt in the pH range 2–10, presumably due to complex formation. Boric acid [$L = B(OH)_4^-$] forms a tetracomplex with Co^{2+}, the log K (stability constant) for CoL_4 being 10.03.[32] Initially, at pH 1, there is little difference in the uptake of cobalt with or without tetraborate anions present. Above pH 2 the sorption of cobalt increases in the presence of tetraborate anions but not to the same degree as observed in plain water. A maximum K_d of about 10 000 mL g^{-1} is achieved at pH 6, compared with 450 000 mL g^{-1} in plain water at the same pH.

In 0.005 M sodium citrate and above pH 8, the uptake of ^{137}Cs by Na-B2 was very similar to that observed in 0.005 M sodium tetraborate (Fig. 6). However, below pH 8 citrate had more effect on the sorption of caesium. The distribution coefficient increased but only to a maximum of about 500 mL g^{-1} at pH 6, and then uptake decreased with decrease in pH. Comparison of Figs. 4 and 6 shows that in the pH range 2–10 the sorption efficiency of Na-B2 for ^{89}Sr in plain water matched closely that for ^{90}Sr/^{90}Y in 0.005 M sodium citrate. Citrate anions had a very large effect on the sorption of trace cobalt by Na-birnessite. Citrate ions (L) form monocomplexes

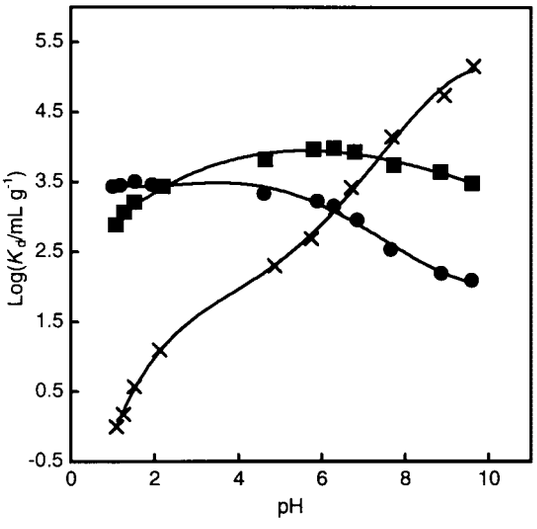

Fig. 5 Distribution coefficients of ^{137}Cs (●), ^{90}Sr/^{90}Y (×) and ^{57}Co (■) on Na-B2 as a function of pH in 0.005 M sodium tetraborate ($V/m = 200$ mL g^{-1}).

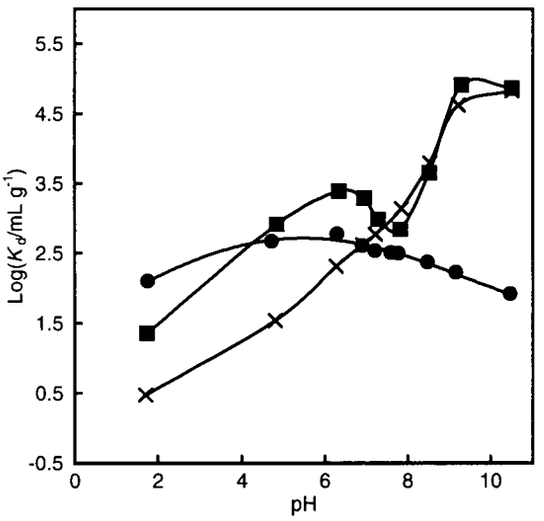

Fig. 6 Distribution coefficients of ^{137}Cs (●), ^{90}Sr/^{90}Y (×) and ^{57}Co (■) on Na-B2 as a function of pH in 0.005 M trisodium citrate ($V/m = 200$ mL g^{-1}).

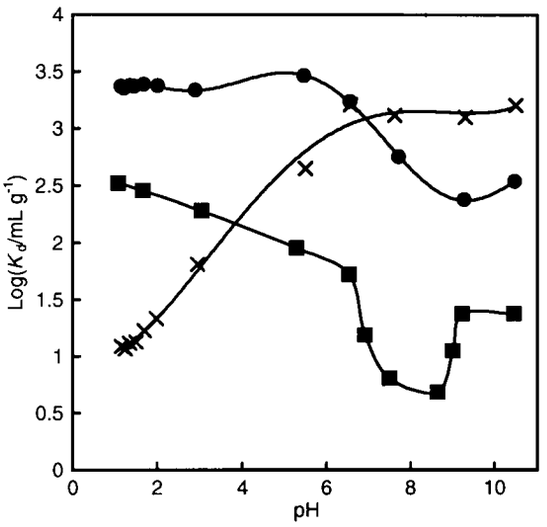

Fig. 7 Distribution coefficients of ^{137}Cs (●), ^{90}Sr/^{90}Y (×) and ^{57}Co (■) on Na-B2 as a function of pH in 0.0001 M disodium EDTA ($V/m = 200$ mL g^{-1}).

with Co^{2+}, the log K for CoL being 5.00. Uptake decreased sharply between pH values of 9 ($K_d = 80\,000$ mL g^{-1}) and 7.75 ($K_d = 750$ mL g^{-1}). It then increased as the pH was lowered, reaching a maximum at equilibrium pH 6.3 ($K_d = 2370$ mL g^{-1}). The distribution coefficient of ^{57}Co then decreased again as the pH was lowered, and at any particular pH was about 200 times lower than that attained in plain water. Only about 0.5% of cobalt ions were removed from solution at equilibrium pH 1.

The sorption behaviour of ^{137}Cs on Na-B2 in 0.0001 M EDTA was similar to that observed in 0.005 M sodium tetraborate. By contrast, EDTA interfered more strongly in the sorption of ^{90}Sr/^{90}Y, especially at high pH. Thus, up to pH 6, performance for ^{90}Sr/^{90}Y was similar to that seen in the presence of tetraborate. Thereafter the uptake levelled off to almost a constant value ($K_d = 2500$ mL g^{-1}). EDTA also had a strong effect on the sorption of trace cobalt, but over a much wider pH range. This was not surprising since it is known that Co(II) forms strong complexes with EDTA. Between pH 11 and 9 the distribution coefficient of ^{57}Co on Na-B2 in 0.0001 M EDTA was 25 mL g^{-1} (11% sorption). Sorption decreased to 5% as the pH was lowered to 8.5 and then increased again to 22% at pH 6.5. This peculiar behaviour is similar to that observed for the sorption of cobalt in the presence of citrate ions. However, as the pH was decreased from 6 to 1, the distribution coefficient increased steadily, approximately linearly on a logarithmic scale. The behaviour at pH > 6 can be attributed to the formation of neutral or negatively charged 1 : 1 complexes between Co(II) ions and EDTA which cannot be sorbed on the surface. As the pH is lowered the exchanger is converted to the hydrogen form and it is likely that sufficient Mn^{2+} ions are released into solution to induce competitive complex dissociation. A second possibility is that sorption of the Co(II)EDTA complex to the birnessite surface increases with a lowering of pH. This kind of behaviour is known to occur with Co(II)EDTA complexes on other oxide surfaces.[35]

Citrate concentration had little effect on the uptake of trace cobalt on Na-birnessite at an equilibrium pH value of about 10.4 (Fig. 8). The distribution coefficient of ^{57}Co on Na-B2 decreased from 140 000 to 100 000 mL g^{-1} when the citrate concentration increased from 10^{-6} M to 10^{-3} M. Tetraborate concentration had a larger effect and the distribution coefficient of ^{57}Co decreased by approximately one order of magnitude in the same concentration range. This behaviour is surprising since the citrate complex with cobalt is stronger than that of borate. It was found previously that citrate concentration had a much stronger effect than tetraborate concentration on the removal of trace cobalt (^{60}Co) by activated carbons, especially at concentrations higher than 10^{-4} M.[32] Fig. 8 clearly demonstrates the strong suppressing effect that EDTA had on trace cobalt uptake, even in very dilute solutions. Thus, the distribution coefficient of ^{57}Co was constant at about 23 mL g^{-1} in the concentration range 10^{-6}–10^{-4} M. It then decreased to 1 mL g^{-1} as the concentration was increased to 0.05 M.

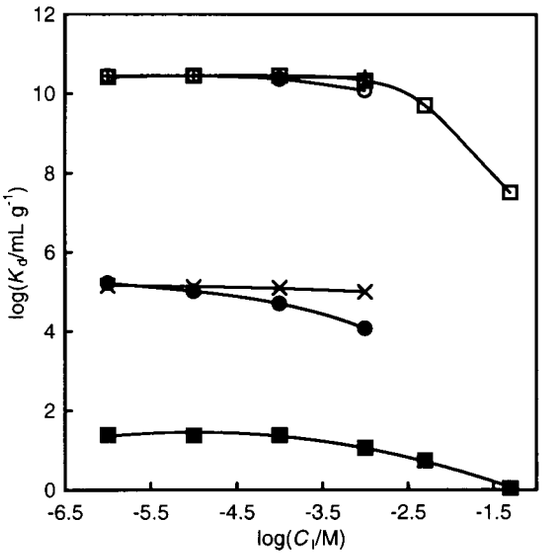

Fig. 8 Distribution coefficient of ^{57}Co on Na-B2 as a function of sodium tetraborate (●), trisodium citrate (×) and disodium EDTA (■) concentrations, and the corresponding equilibrium pH [tetraborate (○), citrate (+), EDTA ■)] ($V/m = 200$ mL g^{-1}).

The Na- and K-birnessite samples with the best sorption efficiencies for trace cobalt ($MnO_4^-/Mn^{2+} = 0.4$, ageing time = 7 days) were tested for the removal of ^{57}Co, ^{137}Cs and ^{89}Sr as a function of pH from a solution that simulated a typical nuclear power plant (NPP) floor drain water (Fig. 9). The simulant had the following components: Na (204 mg L^{-1}), K (20.1 mg L^{-1}), Mg (12.0 mg L^{-1}), Ca (40.1 mg L^{-1}) and NO_3 (675 mg L^{-1}). A large batch factor of 1000 mL g^{-1} was used in order to minimise changes in solution composition during contact with the exchanger. A similar performance was achieved with both materials except in the case of ^{137}Cs when

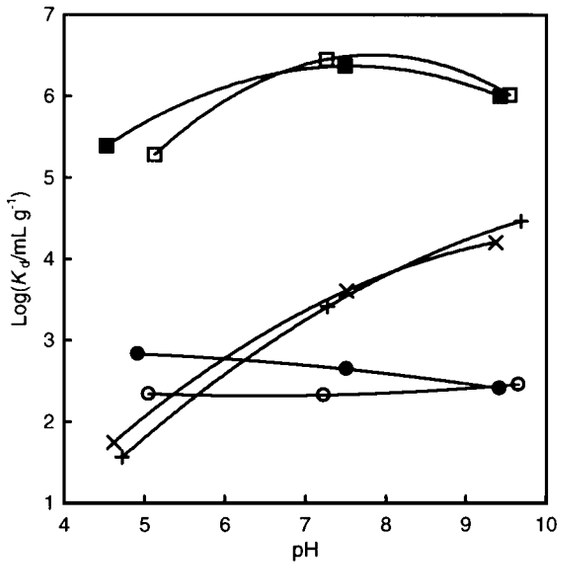

Fig. 9 Distribution coefficients of ^{137}Cs (●), ^{89}Sr (×) and ^{57}Co (■) on Na-B4, ^{137}Cs (○), ^{89}Sr (+) and ^{57}Co (□) on K-B2, as a function of pH in the NPP floor drain water simulant ($Vlm = 1000$ mL g^{-1}).

Na-birnessite was significantly more efficient than K-birnessite at pH values less than 8. Overall the sorption behaviour of the three radionuclides as a function of pH matches that observed in plain water or in 0.1 M $NaNO_3$. Uptake of trace cobalt was highest at about pH 7.5 ($K_d > 10^6$ mL g^{-1}). The distribution coefficient of ^{89}Sr was about three orders of magnitude lower at the same pH. Good performance for trace strontium ($K_d > 10\,000$ mL g^{-1}, 91% sorption) was only achieved at pH values greater than 9.

Summary and conclusions

The synthetic sodium and potassium birnessites studied in this work were highly efficient for the removal of trace cobalt (^{57}Co) across a wide pH range from aqueous solutions containing alkali and/or alkaline earth ions as competing ions. Optimum performance was achieved at equilibrium pH 7–10. The probable uptake mechanism is exchange of cobalt(II) ions with manganese(II) ions at sites located above and below vacancies in the MnO_6 sheet. Cobalt(II) ions may subsequently be oxidised to cobalt(III) and fill vacant positions in the lattice. Complexing agents EDTA, citrate and borate all suppressed trace cobalt sorption across a wide pH range, with EDTA and citrate having the greatest effect. With EDTA, but not citrate, sorption of cobalt increased as the pH was decreased below 7. This was attributed to the release of sufficient Mn^{2+} ions into solution to induce competitive complex dissociation. The manganese oxide sample with the best sorption efficiency for the separation of trace cobalt was prepared under conditions that are known to correlate with the successful synthesis of pure, fully-crystallised birnessite-type layered materials ($MnO_4^-/Mn^{2+} = 0.4$, ageing time of at least 1 week).

Trace caesium and strontium ions were taken up by sodium and potassium birnessites by an ion exchange mechanism involving sodium or potassium ions at sites located on the crystal water sheet. Birnessites are not selective for trace caesium as evidenced by the low selectivity coefficients ($K_{Cs/M} \approx 1$). Performance for strontium was slightly better ($K_{Sr/Na} \approx 75$). Uptake of trace strontium decreased sharply as the equilibrium pH was decreased below 7. The reverse was the case for trace caesium, probably due to a structural change from Na-birnessite to H-birnessite associated with the creation of many more vacancies in the MnO_6 sheet. The sorption of caesium and strontium was not significantly effected by the presence of tetraborate anions. Citrate ions suppressed caesium sorption at low pH and EDTA suppressed trace strontium sorption at high pH, presumably due to complex formation. Sodium birnessite was effective at removing other radionuclides in addition to ^{57}Co (^{63}Ni, ^{54}Mn, ^{59}Fe, ^{65}Zn and ^{236}Pu).

Acknowledgements

This study was funded by the European Commission Framework 4 Nuclear Fission Safety Program (contract FI4W-CT95-0016). We also wish to thank all partners in this contract for helpful discussions.

References

1 *Inorganic Ion Exchange Materials*, ed. A. Clearfield, CRC Press, Boca Raton, Florida, 1982; A. Clearfield, *Ind. Eng. Chem. Res.*, 1995, **34**, 2865.
2 J. Lehto, R. Harjula and A.-M. Girard, *J. Chem. Soc., Dalton Trans.*, 1989, 101.
3 A. I. Bortun, L. N. Bortun, S. A. Khainakov, J. I. G. Alonso, J. R. García and A. Clearfield, *Solvent Extr. Ion Exch.*, 1997, **15**, 895.
4 W. J. Paulus, S. Komarneni and R. Roy, *Nature*, 1992, **357**, 571; T. Kodama and S. Komarneni, *J. Mater. Chem.*, 1999, **9**, 533; T. Kodama and S. Komarneni, *J. Mater. Chem.*, 1999, **9**, 2475.
5 L. N. Bortun, A. I. Bortun and A. Clearfield, in *Ion Exchange Developments and Applications*, ed. J. A. Greig, Royal Society of Chemistry, Cambridge, 1996, p. 313–320.
6 (*a*) S. A. Khan, R. U. Rehman and M. A. Khan, *J. Radioanal. Nucl. Chem.*, 1996, **207**, 19; (*b*) S. A. Khan, R. U. Rehman and M. A. Khan, *Waste Manage.*, 1995, **15**, 641.
7 S. A. Adeleye, R. Rãutiu, D. A. White and P. G. Clay, *J. Mater. Sci.*, 1995, **30**, 583.
8 G. Pacheco, G. N. Galve, P. Bosch and S. Bulbulian, *J. Radioanal. Nucl. Chem.*, 1995, **200**, 259; L. M. Carrera, S. Gómez, P. Bosch and S. Bulbulian, *Zeolites*, 1993, **13**, 622.
9 Q. Feng, H. Kanoh and K. Ooi, *J. Mater. Chem.*, 1999, **9**, 319.
10 S. L. Brock, N. Duan, Z. R. Tian, O. Giraldo, H. Zhou and S. L. Suib, *Chem. Mater.*, 1998, **10**, 2619.
11 (*a*) M. J. Gray and M. A. Malati, *J. Chem. Tech. Biotechnol.*, 1979, **29**, 127; (*b*) M. J. Gray and M. A. Malati, *J. Chem. Tech. Biotechnol.*, 1979, **29**, 135.
12 D. C. Golden, J. B. Dixon and C. C. Chen, *Clays Clay Miner.*, 1986, **34**, 511.
13 M. Tsuji, S. Komarneni, Y. Tamaura and M. Abe, *Mater. Res. Bull.*, 1992, **27**, 741.
14 Q. Feng, H. Kanoh, Y. Miyai and K. Ooi, *Chem. Mater.*, 1995, **7**, 1226.
15 P. Le Goff, N. Baffier, S. Bach and J. P. Pereira-Ramos, *Mater. Res. Bull.*, 1996, **31**, 63.
16 Y. F. Shen, R. P. Zerger, R. N. DeGuzman, S. L. Suib, L. McCurdy, D. I. Potter and C. L. O'Young, *Science*, 1993, **260**, 511.
17 Y. F. Shen, S. L. Suib and C. L. O'Young, *J. Am. Chem. Soc.*, 1994, **116**, 11020.
18 D. C. Golden, C. C. Chen and J. B. Dixon, *Science*, 1993, **231**, 717.
19 R. M. McKenzie, *Aust. J. Soil Res.*, 1970, **8**, 97.
20 P. Loganathan and R. G. Burau, *Geochim. Cosmochim. Acta*, 1973, **37**, 1277.
21 D. L. Crowther, J. G. Dillard and J. W. Murray, *Geochim. Cosmochim. Acta*, 1983, **47**, 1399.
22 A. Manceau, V. A. Drits, E. Silvester, C. Bartoli and B. Lanson, *Am. Miner.*, 1997, **82**, 1150.
23 J. Luo and S. L. Suib, *J. Phys. Chem. B*, 1997, **101**, 10403.
24 J. E. Post and D. R. Veblen, *Am. Miner.*, 1990, **75**, 477.
25 V. A. Drits, E. Silvester, A. I. Gorshkov and A. Manceau, *Am. Miner.*, 1997, **82**, 946; E. Silvester, A. Manceau and V. A. Drits, *Am. Miner.*, 1997, **82**, 962.
26 A. Dyer, M. Pillinger and S. Amin, *J. Mater. Chem.*, 1999, **9**, 2481.
27 A. Dyer and M. Pillinger, in *Advances in Ion Exchange for Industry and Research*, eds. P. A. Williams and A. Dyer, Royal Society of Chemistry, Cambridge, 1999, p. 261.
28 J. Lehto and R. Harjula, *React. Funct. Polym.*, 1995, **27**, 121.
29 R. Harjula, J. Lehto, J. H. Pothuis, A. Dyer and R. P. Townsend, *J. Chem. Soc., Faraday Trans.*, 1993, **89**, 1877.

30 E. M. Mikhail and N. Z. Misak, *Appl. Radiat. Isot.*, 1988, **39**, 1121.
31 S. P. Mishra and D. Tiwary, *Radiochim. Acta*, 1995, **69**, 121.
32 A. Paajanen, J. Lehto, T. Santapakka and J. P. Morneau, *Sep. Sci. Technol.*, 1997, **32**, 813.
33 M. Todorovic, S. K. Milonjic, J. J. Comor and I. J. Gall, *Sep. Sci. Technol.*, 1992, **27**, 671.
34 R. M. McKenzie, *Aust. J. Soil Res.*, 1967, **5**, 235.
35 G. E. Brown, V. E. Henrich, W. H. Casey, D. L. Clark, C. Eggleston, A. Felmy, D. W. Goodman, M. Grätzel, G. Maciel, M. I. McCarthy, K. H. Nealson, D. A. Sverjensky, M. F. Toney and J. M. Zachara, *Chem. Rev.*, 1999, **99**, 77.